Available online at www.sciencedirect.com
SCIENCE DIRECT®
Carbohydrate Research 340 (2005) 75–83
Carbohydrate RESEARCH

Annealing of normal and mutant wheat starches. LM, SEM, DSC, and SAXS studies

Valentina I. Kiseleva,[a] Alexei V. Krivandin,[a] Jozef Fornal,[b] Wioletta Błaszczak,[b] Tomasz Jeliński[b] and Vladimir P. Yuryev[a,*]

[a]*Institute of Biochemical Physics, Russian Academy of Sciences, Kosygina Str. 4, 119991 Moscow, Russia*
[b]*Institute of Animal Reproduction and Food Researches, Polish Academy of Sciences, Tuwima Str. 10, 10-747 Olsztyn, Poland*

Received 5 March 2004; accepted 18 October 2004
Available online 11 November 2004

Abstract—Structure and thermodynamic properties of native and annealed wheat starches with different amylose content (from 1.5% to 39.5%) have been studied by high-sensitivity differential scanning microcalorimetry (HSDSC), small-angle X-ray diffraction (SAXS), light (LM), and scanning electron microscopy (SEM). Starch morphology, the values of the melting cooperative unit, the thickness of crystalline lamellae and the size of amylopectin clusters as well as thermodynamic parameters characterizing surface of the face side in starch crystals were determined. Some suppositions based on different physical approaches are used for a discussion of the results concerning structural reorganization of starches on different levels of macromolecular organization.

Keywords: Normal and mutant wheat starches; Annealing; HSDSC; SAXS; SEM, LM

1. Introduction

It is well known that the structuring of starch granules during biosynthesis of plants is accompanied by development of defects in differently ordered starch structures.[1–6] The amylose 'tie-chains', amylopectin B-chains, molecular ordered structures, that is, double helices located in crystalline lamellae but not participating in a formation of starch crystals, can be considered as such defects.[1–6] An annealing of synthetic imperfect semicrystalline polymers regularizes them. This is followed by narrowing of the melting temperatures interval and by increase in the average melting temperatures. According to theory,[7] these phenomena can be caused by a decrease of the size distribution of crystals and/or by an increase of a cooperative melting unit of crystals. Similar phenomena (an increase of melting temperature and narrowing of melting temperatures intervals) are observed also when starch dispersions in excess water were annealed at temperatures slightly below of the melting temperatures of the starches.[8–10] In the contrast to synthetic polymers, the molecular mechanism of starch annealing is still not clearly understood.

Annealing does not noticeably change the X-ray patterns and size of amylopectin clusters in normal wheat and potato starches.[11–14] Ordinary explanations of the annealing effects on thermodynamic properties are based on the observation of improving of granule stability and reorganization of granular structure.[8–10] Annealing is commonly supposed to improve the crystalline and amorphous lamellae through the optimization of crystalline order.[8–10] However, Nakazawa and Wang[15] observed the defects in annealed starches. It was proposed that the annealing diminishes defects by improvement of double helices registration and optimizes the length of double-helical chains within the crystalline lamellae.[16,17] Recent investigations on the annealing of starches with different polymorphous structures[16,18,19] have shown that small change of crystalline lamellae length causes a significant increase in melting temperature with a small

* Corresponding author. Tel.: +7 095 939 74 42; fax: +7 095 137 41 01; e-mail: v.yuryev@sky.chph.ras.ru

0008-6215/$ - see front matter © 2004 Elsevier Ltd. All rights reserved.
doi:10.1016/j.carres.2004.10.012

increase in melting enthalpies. The total numbers of double helices before and after annealing of wheat starches are similar.[9] Therefore, it was supposed that the new double helices are not formed during annealing, and the optimization of their length takes place due to twisting of unordered ends in preexisting double helices located in the starch crystallites and/or in double helices of molecular ordered structures. It is generally believed that the reorganization of starch molecules during annealing occurs mainly within crystalline lamellae, although considerable evidence in favor of this suggestion was obtained in the studies of potato[19] and barley[16] starches, only.

A fraction of the increase of melting temperatures can be caused by a change in amorphous lamellae. In particular, a conformation of defects (unordered amylopectin B-chains and part of amylose tie-chains) locating in amorphous lamellae becomes energywise favorable due to annealing. Furthermore, according to Liu and Lelievre[20] a narrowing of the temperature melting interval during the annealing of starches[8] can be due to changes in sizes of starch granules. Consequently, it can be supposed that structural variations observed at annealing affect the higher levels of structural organization rather than the crystalline and amorphous lamella. At present there are, as minimum, three levels of structural organization namely: granular (μm), clusters (~10 nm), and lamellar (~4–6 nm) levels. The granular level can be studied using LM and SEM. The clusters level is usually studied by the SAXS method, whilst HSDSC can be used for studying of the lamellar level.

Recently, wheat starches with amylose content ranging from 0.2% to 39.5% have been investigated.[21–23] The DSC, SAXS, and SEM investigations of wheat starches with different amylose content have shown that the increase of amylose content in granules leads to the structural changes on the different levels of starch macromolecular organization, particularly due to the accumulation of defects that are likely to locate both in crystalline and amorphous lamellae.[23,24] On the other hand, annealing of mutant wheat starches has not been adequately explored. While DSC and SAXS provide the valuable data on reorganization in crystalline and amorphous lamellae,[23,24] SEM allows one to detect the morphological changes of starch granules during annealing. In this paper, the annealing effects on the structure of granules of wheat starches with different amylose content are investigated by means of DSC, SAXS, and SEM methods.

2. Experimental

2.1. Materials

Wheat varieties (*Imeni* (*im.*) *Rapoporta*, *Bulava*) were selected through chemical mutagenesis, using ethyleneimine (aziridine) as a mutagen. The wheat varieties investigated were grown in Central Russia (Moscow's Region) in the 2000 season. Native starches were isolated according to Richter et al.[25] The starch from '*Leona*' wheat variety was kindly supplied by Dr. P. Seib. The amylose content of starches has been determined elsewhere[23,24] according to a standard method.[25] The amylose content of three wheat starch cultivars was as follows: '*Leona*'—1.5%, '*im. Rapoporta*'—26.0%, and '*Bulava*'—39.5%.

The annealing procedure for starches has been described in the literature.[19] The annealing temperatures (incubation temperatures) were chosen slightly (2–3 K) below the onset melting temperature (T_o) of native starches. The annealing temperatures for starches investigated are shown in Figure 6 (see part 'Results and discussion').

2.2. Methods

2.2.1. High-sensitivity differential scanning microcalorimetry (HSDSC). Calorimetric investigations of 0.3–0.5% dispersions of starch in water (0.5 cm^3) placed in the sealed cells were performed using a DASM-4 (Puschino, Russia) high-sensitivity differential scanning microcalorimeter. The temperature interval was between 10 and 120 °C. The heating rate was 2 K/min. The excess pressure was 2.5 bar. The heat capacity was calibrated using the Joule–Lenz effect for each run. Corrections for dynamic lag and residence of the samples in the calorimetric cell were not necessary[26,27] under conditions used in our experiments. The average values of the thermodynamic parameters were determined as described elsewhere.[26–28] The error in measurements of melting temperature and melting enthalpy were ±0.1 K and ±0.3 kJ/mol, respectively.

The magnitudes of the van't Hoff enthalpy (ΔH^{vH}) were calculated according to the methods reported.[26–29] In the case of starches with symmetrical DSC endotherms, the sizes of the melting cooperative units (v) and the thicknesses of the crystalline lamellae (L_{crl}) were calculated according to Eqs. 1 and 2.[1–3,26–28]

$$v = \Delta H^{vH}/\Delta H_m \quad (1)$$

where ΔH_m is the melting enthalpy of crystalline lamellae.

$$L_{crl} = 0.35v \quad (2)$$

where, according to,[30] there is pitch height of 0.35 nm per anhydroglucose residue in the double helices.

According to our paper,[28] the degree of polymerization of amylopectin A-chains in double helices of annealed starch ($N_2 = v_{an.st.}$) can be also calculated using Eqs. 3 and 4:

$$N_2 = N_1 + \Delta N \quad (3)$$

where $N_1 = \nu_{\text{native starch}}$ is the degree of polymerization of amylopectin A-chains in double helices of native starch; ΔN is the difference in the degree of polymerization of amylopectin A-chains between the annealed and native starches.

$$\Delta N = (\Delta T \cdot c \cdot \nu_{\text{native starch}})/T_{\text{m.native starch}} \quad (4)$$

where c is the constant equal[28] to 28, ΔT is the difference in the melting temperatures of the annealed and native starches.

In the case of symmetric DSC endotherms, the Thomson–Gibbs' equation 5[7] was applied to calculate the thermodynamic parameters characterizing surface properties of the crystalline lamellae.

$$T_{\text{m}} = T^{\circ}_{\text{m}}[1 - 2\gamma_i/(\Delta H^{\circ}_{\text{m}}\rho_{\text{crl}}L_{\text{crl}})] \quad (5)$$

where T°_{m} and $\Delta H^{\circ}_{\text{m}}$ are the melting temperatures and melting enthalpies of a perfect crystals of unlimited sizes, γ_i is the free surface energy of the face sides of the crystal, ρ_{crl} and L_{crl} are the densities and the thicknesses of the crystals. Parameter γ_i may be calculated using Eqs. 5–7:

$$q_i = [(\Delta H^{\circ}_{\text{m}} - \Delta H_{\text{m}})L_{\text{crl}}\rho_{\text{crl}}]/2.5 \quad (6)$$

and

$$\gamma_i = q_i - T_{\text{m}}s_i \quad (7)$$

where q_i and s_i are the surface enthalpy and surface entropy of the crystal, respectively.

Since the melting temperature (T°_{m}) and melting enthalpy ($\Delta H^{\circ}_{\text{m}}$) for perfect crystal are not available, $T^{\circ}_{\text{m}} = 366.5$ K and $\Delta H^{\circ}_{\text{m}} = 35.5$ J/g, known for A-type spherolitic crystals,[31] were used instead. L_{crl}, ΔH_{m}, and T_{m} are given in Table 1, and $\rho_{\text{crl}} = 1.48$ g/cm^2[,31] was taken as that for A-type structures.

2.2.2. Small-angle X-ray scattering (SAXS). Slurries of native starch powder in excess of distilled water were used in the SAXS experiments. The SAXS measurements were carried out in the transmission geometry mode using an X-ray diffractometer designed in the Institute of Biochemical Physics. The starch slurries were kept in the sealed cells to prevent the dehydration during the X-ray exposure. The X-ray beam emitted from the fine focus Cu X-ray tube operating at 30 kV/30 mA was Ni-filtered and line-focused with a glass mirror collimator of the Franks type.[32] The SAXS patterns were recorded with a gas-filled (85% Xe, 15% Me), one-dimensional position-sensitive detector with a delay line readout constructed in JINR.[33] The sample-to-detector distance was 415 mm. Experimental SAXS curves were corrected for the background scattering, desmeared by the method[34] and plotted as a function of $S = (2\sin\theta)/\lambda$, λ and θ being the Cu K_α-wavelength (0.1542 nm) and a half of the scattering angle, respectively. The Bragg spacing D (the thickness of amylopectin cluster) was calculated according to the Woolf–Bragg's equation as $D = 1/(S_{\max})$, where $S_{\max}$ is the position of the SAXS peak.

2.2.3. Light (LM) and scanning electron microscopy (SEM). Starches were suspended in distilled water (8% w/w), and the suspension was poured on a microscopic glass was observed in an LM microscope (OLYMPUS BX60) with polarized light using Nomarski contrast.[35] In the case of SEM, dry granules were deposited on a copper disc and coated with gold using the Jeol JEE-400 vacuum evaporator. The specimens were examined by means of the scanning electron microscope (Jeol 5200) at 10 kV accelerating voltage.

To study the internal structure, native or annealed starch granules were preliminarily treated in hydrochloric

Table 1. The values of amylose content in wheat starches, the annealing time ($\tau_{\text{annealing}}$), the melting temperature (T_{crl}), enthalpy (ΔH_{crl}) and melting range of crystalline lamellae (ΔT_{crl}), melting temperature (T_{alc}) and enthalpy (ΔH_{alc}) of amylose–lipid complexes

Genotype	Amylose content (%)	$\tau_{\text{annealing}}$ (h)	T_{crl} (K)	ΔH_{crl} (kJ/mol)	ΔT_{crl} (K)	T_{alc} (K)	ΔH_{alc} (kJ/mol)
Leona	1.5	0	336.6	2.8	11.8	362.9	0.2
		0.5	336.6	2.8	11.2	363.0	0.2
		1.5	336.8	3.0	11.2	363.0	0.1
		4	337.3	3.5	9.2	363.0	0.2
		10	338.2	3.3	7.0	363.0	0.2
im. Rapoporta	26.0	0	330.5	2.3	13.5	363.2	0.3
		0.5	330.6	2.4	12.6	366.2	0.5
		1.5	330.8	2.3	11.6	366.3	0.6
		4	331.0	1.9	10.1	366.2	0.3
		10	331.4	2.4	8.6	365.9	0.2
Bulava	39.5	0	329.7	2.5	14.1	366.8	0.4
		0.5	333.0	2.3	10.9	365.0	0.3
		1.5	333.0	2.2	9.4	364.5	0.4
		4	333.3	2.3	8.8	364.4	0.3
		10	333.8	2.4	7.5	364.4	0.3

acid before the SEM investigations. Starch granules (50 mg, d.w.) were treated in 3 mL of 8% (2.2 N) hydrochloric acid in a 30-mL centrifuge sealed tube. The tubes were continuously and gently shaken in a water bath at 38 °C for 12 h. After addition of 15–20 mL of cold distilled water, the tubes were centrifuged. The supernatant was discarded, and the starch residue (a pellet) was washed until neutral and finally dried in an oven at 25 °C.

3. Results and discussion

SEM and LM pictures of the investigated wheat starches are presented in Figures 1–4. These pictures show that the annealing of amylopectin (Fig. 1C and D)—*Leona* variety) and high-amylose (Fig. 2C and D—*Bulava* variety) starches is not accompanied by significant changes in the granular morphology.

However, in contrast to the native starches (photos not shown), small deformations and out-of-the-*xy*-plane puckering of the lens-shaped granules are observed. It is worthwhile to note that the granules of the high-amylose starch were deformed more markedly than granules of amylopectin starch. After annealing, the concentric growth rings and Maltese-cross structures remain unchanged in the LM of the investigated starches (Fig. 3A and B and Fig. 4A and B). This means that the granular and lamellar starch structures remain intact.

It is well known[15] that the hydrolysis of the amorphous background is the first stage of acidic treatment. This promotes a visualization of the internal structure of the granules in microscopic investigations. SEM pictures of native and annealed starches after acidic treatment showed alternating light and dark layers, the former being related to semicrystalline growth rings, the latter to the amorphous background. As it is seen from Figure 2A and B and Figure 2E and F, for the high-amylose starches (*Bulava* variety), the density of alternating structures seems to be higher for the annealed starches than for the native ones. Moreover, the acidic treatment of the annealed amylopectin (*Leona* variety)

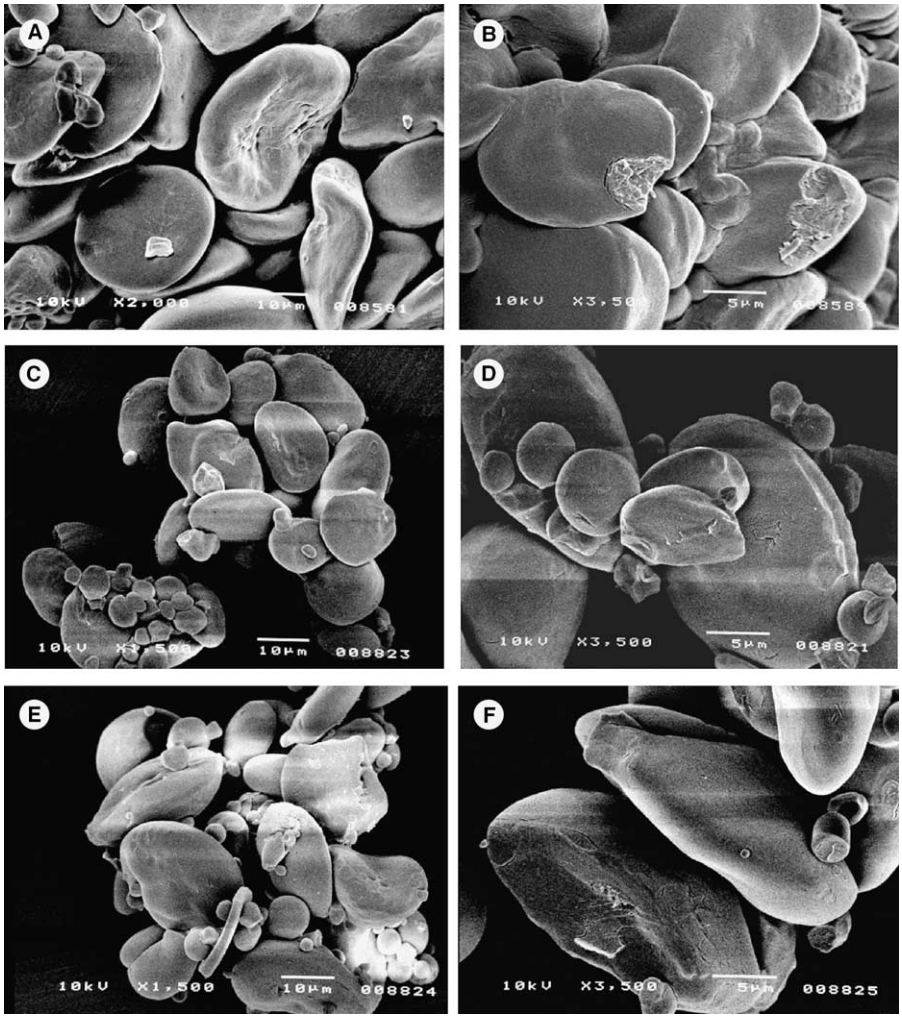

Figure 1. SEM pictures of *Leona* starch after: (A, B) control + HCl treatment; (C, D) annealing; (E, F) annealing + HCl treatment.

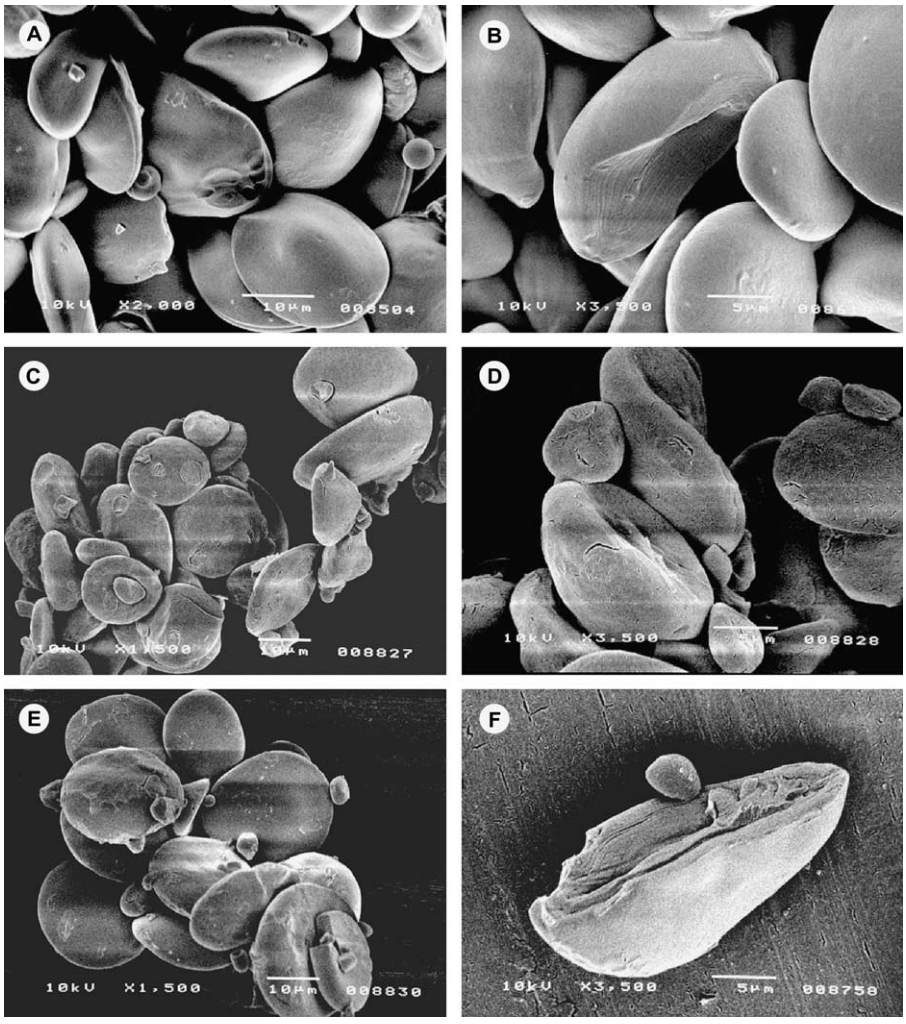

Figure 2. SEM pictures of *Bulava* after: (A, B) control + HCl treatment; (C, D) annealing; (E, F) annealing + HCl treatment.

starches (Fig. 1E and F) did not reveal the structures related to semicrystalline growth rings and the amorphous background. This can be explained by formation of the denser structures generated by annealing. In their turn, the denser structures prevent penetration of an acid into the granules. Semicrystalline growth rings consist of an amylopectin cluster. Therefore, the perfection of structure in clusters gains during annealing.

The SAXS curves obtained on the amylopectin starch clusters are presented in Figure 5.

As is evident from Figure 6, the SAXS curves for native and annealed starches are similar. Calculated according to the Woolf–Bragg's equation, the thickness of the amylopectin clusters equals approximately to 10 nm and does not depend on the amylose content in the starches. This accords well with the results[14] on potato starch. The calculations[24] as applied to the paracrystalline model gave the sizes of amylopectin clusters being within an interval of 9.1–9.15 nm. We failed to find noticeable differences in the thickness of crystalline lamella for native and annealed starches.

The DSC traces and the melting characteristics of native and annealed starches are presented in Figure 6 and Table 1, respectively. It is seen from these data that the increase in annealing time narrows down the temperature melting interval and increases the melting temperature of the crystalline lamella. The effect maximizes at 10 h of annealing and does not depend on the amylose content in starches.

These results well agree with the data for potato,[19] barley,[16,17] and sweet potato[18] starches. Moderate changes in melting temperatures for amylopectin and normal wheat starches are practically the same as those observed by Nakazawa and Wang for normal wheat starches[15] incubated during 24 h at an annealing temperature of 40 °C.

As it follows from the research of semicrystalline synthetic polymers,[7] the type of polymorphous structure and the thickness of crystalline lamellae influence the melting temperature of ordered structures. Wheat starches contain only A-type structures[2] irrespective of amylose content. So, it is necessary to consider the

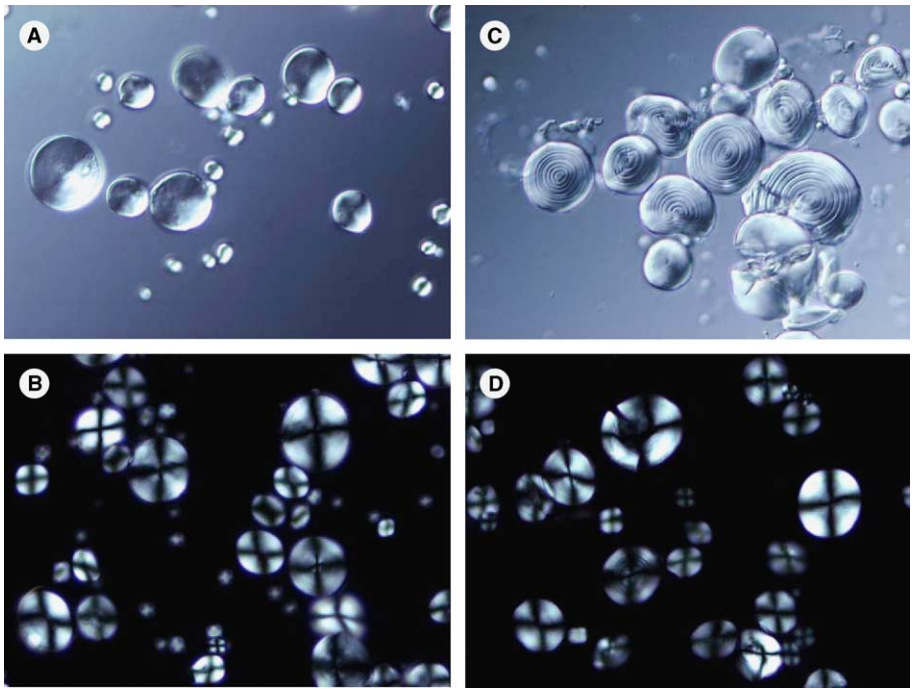

Figure 3. LM pictures of *Leona* starch after: (A, B) annealing; (C, D) annealing + HCl treatment.

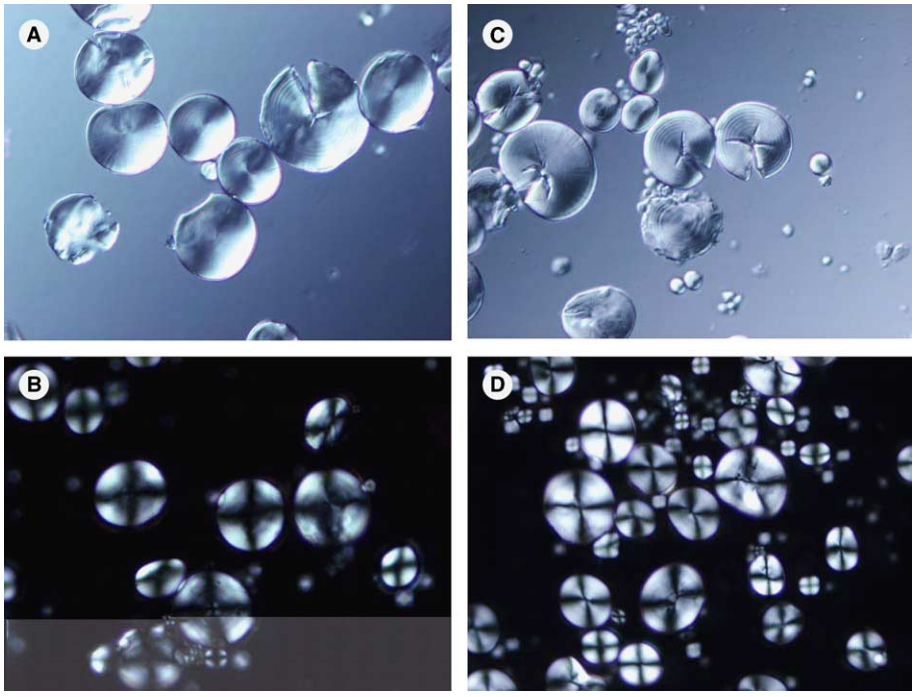

Figure 4. LM pictures of *Bulava* starch after: (A, B) annealing; (C, D) annealing + HCl treatment.

changes in the thicknesses of crystalline lamellae during the annealing of the starches.

Cooperative melting units were calculated using Eqs. 1 and 2 as applied to the 'two-state' model.[26–28] As it follows from Table 2, the cooperative melting units and the thicknesses of the crystalline lamellae increase with the annealing time for all investigated starches. The same parameters were calculated from Eqs. 3 and 4 according to the model where an increment of the melting temperature is the function of length of starch double helixes.[28]

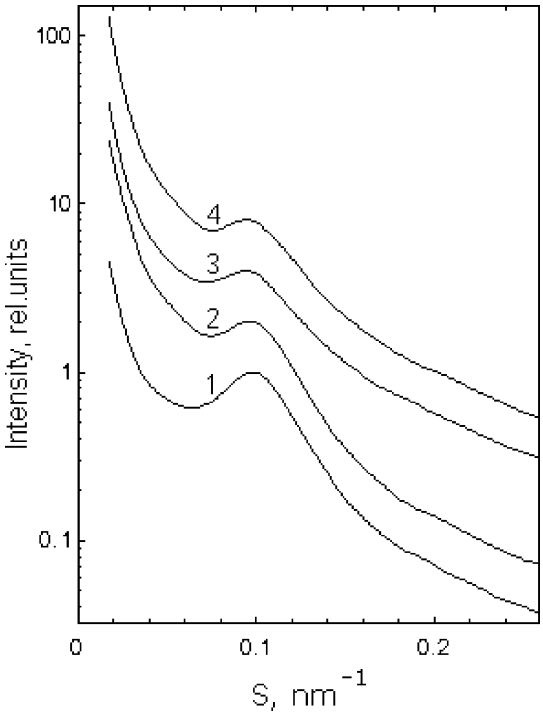

Figure 5. SAXS curves for the native and annealed wheat starches. The curves: (1, 3) native starches from *Leona* and *Bulava* cultivars; (2, 4) annealed starches (10 h annealing) from *Leona* and *Bulava* cultivars. The curves were arbitrary shifted in the vertical direction.

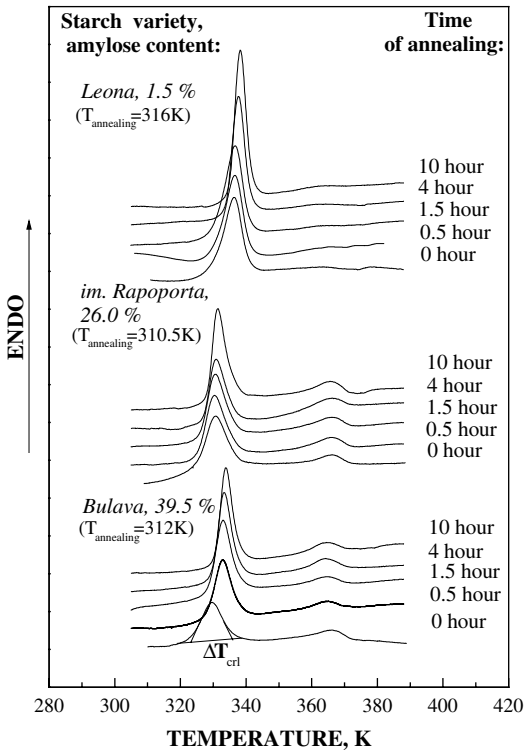

Figure 6. DSC traces of native and annealed wheat starches of different amylose content.

The results given by two approaches are practically the same. Consequently, the annealing of starches is accompanied by an increase in cooperative melting unit and the corresponding increase in the thickness of the crystalline lamellae. A lengthening of the amylopectin A-chains in amylopectin and normal wheat starches is within a range of 1.7–2.4 anhydroglucose residues. For the high-amylose wheat starches, this interval is 5.7 anhydroglucose residues. These results are quite expected since the content of defects in the high-amylose wheat starches exceeds that in the amylopectin and normal wheat starches.[23,24]

It was supposed that an additional twisting of the amylopectin A-chains can take place in the molecular ordered structures and double helices appurtenant to

Table 2. The values of the cooperative melting ($\nu_{crl.eq.1,2}$) unit and the thickness of crystalline lamellae ($L_{crl.eq.1,2}$) calculated according to Eqs. 1 and 2 as well as of the cooperative melting ($\nu_{crl.eq.3,4}$) unit and the thickness of crystalline lamellae ($L_{crl.eq.3,4}$), calculated according to Eqs. 3 and 4, for native and annealed wheat starches

Genotype	Amylose content (%)	$\tau_{annealing}$ (h)	$\nu_{crl.eq.1,2}$ anhydroglucose residues	$L_{crl.eq.1,2}$ (nm)	$\nu_{crl.eq.3,4}$ anhydroglucose residues	$L_{crl.eq.3,4}$ (nm)
Leona	1.5	0	12.7	4.5	12.7	4.5
		0.5	13.9	4.9	12.7	4.5
		1.5	13.5	4.7	12.9	4.5
		4	12.9	4.5	13.5	4.7
		10	15.8	5.5	14.8	5.2
im. Rapoporta	26.0	0	13.9	4.9	13.9	4.9
		0.5	13.9	4.9	14.0	4.9
		1.5	14.9	5.2	14.3	5.0
		4	17.8	6.2	14.7	5.1
		10	16.6	5.8	15.2	5.3
Bulava	39.5	0	12.1	4.7	12.1	4.7
		0.5	15.6	5.5	16.4	5.8
		1.5	16.4	5.7	16.7	5.8
		4	17.4	6.1	17.4	6.1
		10	17.7	6.2	18.2	6.4

crystallites. The increase of the thickness of the crystalline lamellae (Table 2) most probably will be observed in the case of initially unordered ends of amylopectin A-chains belonging to most lengthy crystallites that define the size of crystalline lamellae.

The increase in the length of the double helices in annealed starches is confirmed by the increase in the melting enthalpy of the amylopectin wheat starches (Table 1). These changes are due to formation of the new hydrogen bonds in additional turns of the helix. So, one can suppose that the annealing of amylopectin wheat starches is accompanied by the twisting of unordered ends appurtenant to longer crystallites and located in the amorphous lamellae. This leads to an increase in the thickness of the crystalline lamellae, and as a consequence,[7] to an increase in the melting temperature of annealed starches. Moreover, we have observed the decrease in the entropy of the surface of the face side of the crystals (Table 3), and this decrease was proportional to a content of defects.[7] At the same time, the lengthening of molecular ordered structures and short crystallites cannot be excluded.

Since the lengthening of double-helical chains in the high-amylose starches reaches 5.7 anhydroglucose residues, that is, is 2.4–3.3 times larger than that in the amylopectin and normal wheat starches, the most significant changes in ΔH_{crl} during annealing of high-amylose wheat starch can be expected. However, as can be seen from Table 1, the ΔH_m in the annealed starches remains practically intact. The main contribution to the ΔH_m of starches as well as synthetic polymers[7] is believed to be carried by melting of the hydrogen bonds that stabilize the double helices. Therefore, the lengthening of the double-helical chain formed from the A-chains and the increase in the thickness of the crystalline lamellae during the annealing of high-amylose starches (Table 2) is caused by the additional coiling of the defective ends of the double-helical chains and/or crystallization of pre-existing double helices but not participating in formation of crystals in native starches. In this case, formation of crystals is determined[7] by a disturbance of the position and orientation but not conformation orders. The increase of annealing time for this case is accompanied by the increase in the formation entropy (Table 3) for the surface of the face side in the starch crystallites (Table 3).

The array of data on the normal wheat starches from *im. Rapoporta* variety (insignificant increase in the v_{crl} and the L_{crl}, $\Delta H_{crl} \approx 0$; the increase in the s_i (Tables 1 and 2)) suggests that the observed changes (Tables 1–3) in starches caused by annealing are intermediate between those in amylopectin and high-amylose wheat starches.

DSC and SAXS data indicate that the annealing of starches provides the changes in the sizes of the crystalline and amorphous lamellae (Tables 2 and 3). At the same time, the total size of the amylopectin clusters remains unchanged (Fig. 5).

In contrast to the molecular reorganization in the crystalline lamellae that is caused by annealing, the melting parameters of the amylose–lipid complexes are insignificantly varied (Table 1). This agrees well with similar results obtained in the recent study of barley starches.[16] Because of the known relationships between structural and thermodynamic parameters of starches,[1–6,16–20,23] the insignificant change in the melting parameters of the amylose–lipid complexes means that the annealing does not substantially influence the structure of the amylose–lipid complexes.

Table 3. Surface free energy (γ_i), enthalpy (q_i), and entropy (s_i) of crystalline lamellae in native and annealed wheat starches

Genotype	Amylose content (%)	$\tau_{annealing}$ (h)	γ_i (J/cm^2) 10^7	q_i (J/cm^2) 10^7	s_i (J/cm^2 K) 10^7
Leona	1.5	0	10.07	50.7	0.121
		0.5	10.41	52.21	0.124
		1.5	10.06	48.20	0.113
		4	9.46	36.56	0.080
		10	11.19	48.44	0.110
im. Rapoporta	26.0	0	12.13	59.7	0.143
		0.5	12.54	59.18	0.141
		1.5	13.38	66.41	0.160
		4	15.81	88.28	0.219
		10	14.57	70.19	0.168
Bulava	39.5	0	12.4	57.57	0.137
		0.5	13.12	69.36	0.169
		1.5	13.76	73.39	0.179
		4	14.50	77.76	0.190
		10	14.51	76.99	0.187

4. Conclusions

The annealing of wheat starches with different amylose content is accompanied by the insignificant changes in the morphology of the starch granules and the formation of more perfect starch crystals. Crystals of the native starches with higher defect content[23,24] (high-amylose starches) suffer more essential reorganization than starches with lower defect content[23,24] (amylopectin and normal starches). The mechanisms of reorganization in high-amylose and amylopectin starches are different. For the amylopectin wheat starches, annealing leads to an insignificant lengthening of the amylopectin A-chains and to an increase in the thicknesses of the crystals. This is due to the twisting of the unordered free ends appurtenant to longer crystallites. For the high-amylose starches, the annealing is accompanied by a significant increase in the thicknesses of the crystals due to intermolecular interactions between double helices already existing in the crystalline lamellae. Irrespective

of amylose content in the starches, these processes do not lead to changes in the size of the amylopectin clusters.

The thermodynamic melting parameters of the amylose–lipid complexes are insignificantly varied. The relationship between the structural and thermodynamic parameters for starches[1–6,16–20,23] suggests that annealing does not influence the structure of the amylose–lipid complexes.

References

1. Protserov, V. A.; Karpov, V. G.; Kozhevnikov, G. O.; Wasserman, L. A.; Yuryev, V. P. *Starch/Stärke* **2001**, *52*, 461–466.
2. Wasserman, L. A.; Eiges, N. S.; Koltysheva, G. I.; Andreev, N. R.; Karpov, V. G.; Yuryev, V. P. *Starch/Stärke* **2001**, *53*, 629–634.
3. Protserov, V. A.; Wasserman, L. A.; Tester, R. F.; Debon, S. J. J.; Ezernitskaja, M. G.; Yuryev, V. P. *Carbohydr. Polym.* **2002**, *49*, 271–279.
4. Kiseleva, V. I.; Tester, R. F.; Wasserman, L. A.; Krivandin, A. V.; Popov, A. A.; Yuryev, V. P. *Carbohydr. Polym.* **2003**, *51*, 407–415.
5. Yuryev, V. P.; Genkina, N. K.; Wasserman, L. A. *Żywność* **2002**, *9* (Supl.), 153–168.
6. Yuryev, V. P.; Wasserman, L. A. In *Biochemistry and Chemistry*; Zaikov, G. E., Lobo, V. M. M., Eds.; Nova Science: New York, 2003; Chapter 7, pp 91–114.
7. Bershtein, V. A.; Egorov, V. M. In *Differential Scanning Calorimetry of Polymers. Physics, Chemistry, Analysis, Technology*; Kemp, T. J., Ed.; Ellis Horwood: New York, 1994; pp 1–253.
8. Jacobs, H.; Delcour, J. A. *J. Agric. Food Chem.* **1998**, *46*, 2895–2905.
9. Tester, R. F.; Debon, S. J. J.; Karkalas, J. *J. Cereal Sci.* **1998**, *28*, 259–272.
10. Kulp, K.; Lorenz, K. *Cereal Chem.* **1983**, *58*, 46–48.
11. Stutte, R. H. *Starch/Stärke* **1992**, *44*, 205–214.
12. Gouch, B. M.; Pybus, J. N. *Starch/Stärke* **1971**, *23*, 210–212.
13. Lorenz, K.; Kulp, K. *Starch/Stärke* **1980**, *32*, 181–186.
14. Jacobs, H.; Mischenko, N.; Koch, M. H. J.; Eerlingen, R. C.; Delcour, J. A.; Reynaers, H. *Carbohydr. Res.* **1997**, *306*, 1–10.
15. Nakazawa, Y.; Wang, Y.-J. *Carbohydr. Res.* **2003**, *338*, 2871–2882.
16. Kiseleva, V. I.; Genkina, N. K.; Tester, R. F.; Wasserman, L. A.; Popov, A. A.; Yuryev, V. P. In *Starch: from Polysaccharides to Granules, Simple and Mixtures Gels*; Yuryev, V. P., Tomasik, P., Ruck, H., Eds.; Nova Science: New York, 2004; Chapter 10, pp 147–168.
17. Qi, X.; Tester, R. F.; Snape, C. E.; Yuryev, V. P.; Wasserman, L. A.; Ansell, R. *J. Cereal Sci.* **2004**, *39*, 57–66.
18. Genkina, N. K.; Wasserman, L. A.; Noda, T.; Tester, R. F.; Yuryev, V. P. *Carbohydr. Res.* **2004**, *339*, 1093–1098.
19. Genkina, N. K.; Wasserman, L. A.; Yuryev, V. P. *Carbohydr. Polym.* **2004**, *56*, 367–370.
20. Liu, H.; Lelievre, J. *Carbohydr. Polym.* **1993**, *20*, 1–5.
21. Yusui, Y.; Matsuki, J.; Sasaki, J.; Yamamori, M. *J. Cereal Sci.* **1996**, *24*, 131–140.
22. Graybosch, R. A. *Trends Food Sci. Technol.* **1998**, *9*, 135–142.
23. Bocharnikova, I.; Wasserman, L. A.; Krivandin, A. V.; Fornal, J.; Błaszczak, W.; Chernykh, V. Ya.; Schiraldi, A.; Yuryev, V. P. *J. Thermal Anal. Calorim.* **2003**, *74*, 681–695.
24. Yuryev, V. P.; Krivandin, A. V.; Kiseleva, V. I.; Wasserman, L. A.; Genkina, N. K.; Fornal, J.; Błaszczak, W.; Schiraldi, A. *Carbohydr. Res.* **2004**, *339*, 2683–2691.
25. Richter, M.; Augustadt, S.; Schierbaum, F. *Ausgewahlte Methoden der Stärkechemie*; VEBFachbuch: Leipzig, 1968.
26. Danilenko, A. N.; Shtikova, Ye. V.; Yuryev, V. P. *Biophysics* **1994**, *39*, 427–432.
27. Andreev, N. R.; Kalistratova, E. N.; Wasserman, L. A.; Yuryev, V. P. *Starch/Stärke* **1999**, *51*, 422–429.
28. Matveev, Y. I.; Soest, J. J. G.; Niemann, C.; Wasserman, L. A.; Protserov, V. A.; Ezernitskaja, M.; Yuryev, V. P. *Carbohydr. Polym.* **2001**, *44*, 151–160.
29. Privalov, P. L.; Khechinashvili, N. N. *J. Mol. Biol.* **1974**, *86*, 665–684.
30. Gernat, Ch.; Radosta, S.; Anger, H.; Damaschun, G. *Starch/Stärke* **1993**, *45*, 309–314.
31. Whittam, M. A.; Noel, T. R.; Ring, S. In *Food Polymers, Gels and Colloids*; Dickenson, E., Ed.; Royal Society of Chemistry: Cambridge, 1991; pp 277–288.
32. Franks, A. *Br. J. Appl. Phys.* **1958**, *9*, 349–352.
33. Cheremukina, G. A.; Chernenko, S. P.; Ivanov, A. B.; Pashekhonov, V. D.; Smykov, L. P.; Zanevsky, Yu. V. *Isotopenpraxis* **1990**, *26*, 547–549.
34. Shedrin, B. M.; Feigin, L. A. *Kristallografia* **1966**, *11*, 159–163 (in Russian).
35. Błaszczak, W.; Valverde, S.; Fornal, J.; Amarowicz, R.; Lewandowiz, G.; Borkowski, K. *Carbohydr. Polym.* **2003**, *53*, 63–73.